

Accelerating Molecular Dynamics Simulations with Foundation Neural Network Models using Multiple Time-Step and Distillation

Côme Cattin,[†] Thomas Plé,^{*,†} Olivier Adjoua,[†] Nicolai Gouraud,[‡] Louis
Lagardère,[†] and Jean-Philip Piquemal^{*,†}

[†]*Sorbonne Université, Laboratoire de Chimie Théorique, UMR 7616 CNRS, 75005 Paris,
France*

[‡]*Qubit Pharmaceuticals, Advanced Research Department, 75014 Paris, France*

E-mail: thomas.ple@sorbonne-universite.fr; jean-philip.piquemal@sorbonne-universite.fr

Abstract

We present a strategy to accelerate molecular dynamics simulations using foundation neural network models. To do so, we apply a dual-level neural network multi-time-step (MTS) strategy where the target accurate potential is coupled to a simpler but faster model obtained via a distillation process. Thus, the 3.5 Å-cutoff distilled model is sufficient to capture the fast varying forces, i.e. mainly bonded interactions, from the accurate potential allowing its use in a reversible reference system propagator algorithms (RESPA)-like formalism. The approach conserves accuracy, preserving both static and dynamical properties, while enabling to evaluate the costly model only every 3 to 6 fs depending on the system. Consequently, large simulation speedups over standard 1 fs integration are observed: 4-fold in homogeneous systems and 2.3-fold in large solvated proteins. Such a strategy is applicable to any neural network potential and reduces their performance gap with classical force fields.

Introduction

Neural Network potentials (NNPs) ¹⁻¹⁵ have emerged as powerful tools to perform molecular dynamics (MD) simulations, offering near-quantum mechanical accuracy at a fraction of the computational cost of *ab initio* methods. Presently, such models can be generalized up to Foundation Models covering complete area of applications of molecular dynamics ranging from Material Science to Chemistry, Biology and Drug Design.¹⁶⁻²⁰ By learning the potential energy surface from reference quantum chemistry data, these models enable simulations of large and complex molecular systems with significantly improved fidelity compared to classical force fields.²¹ However, this increase in accuracy comes at a cost: NNPs are substantially more expensive to evaluate than traditional empirical potentials. This limits their applicability in term of system sizes and long-timescale simulations.

One of the primary bottlenecks of performing MD with ML potentials lies in the time integration itself. The equations of motion must be solved with a small time step - typically in the order of 0.5 to 1 femtosecond - to resolve high-frequency motions such as bond vibrations. With computationally intensive ML models, this results in a high number of expensive force evaluations, further amplifying the overall simulation cost.

Multi-Time-Step (MTS) integrators²²⁻²⁴ offer a well-established strategy to address this challenge. Originally introduced in the context of classical molecular simulations, MTS methods such as RESPA (Reference System Propagator Algorithm)²² exploit the separation of timescales between different components of the forces to reduce the number of expensive evaluations. By integrating fast-changing forces with a small time step and slow-changing ones with a larger time step, significant performance gains can be achieved without compromising accuracy.

Despite their proven utility in classical force fields, MTS schemes have not yet been adapted to the context of ML-based force field to the best of our knowledge. Indeed, in this context force decomposition is not naturally given by physical interactions. This represents an important opportunity: the use of multiple neural networks of differing complexity and

inference cost could enable efficient MTS schemes specifically tailored to ML potentials.

In this work, we propose the first implementation of a RESPA-based MTS scheme for ML potentials. We integrate this approach into the FeNNol library,²⁵ a neural network framework for molecular simulations that can be coupled to the scalable Deep-HP machine learning interface²⁶ present in the GPU-accelerated Tinker-HP molecular dynamics package.^{27,28} Our method associates a small, fast NNP to the FeNNix-Bio1(M) foundation model,¹⁹ leveraging the speed of the former to reduce the frequency of the expensive evaluations of the latter. We systematically evaluate the method using various systems including water solvent, solvated small molecules and proteins in the condensed phase, exploring different hyperparameter settings and model sizes in order to design the fastest setup while maintaining accuracy. We also assess the use of a foundation model as a general-purpose fast component to improve transferability across system.

Our results show that this hybrid RESPA-like scheme enables substantial computational speed-ups with limited loss of accuracy, offering a practical route to scalable and efficient Molecular Dynamics with foundation machine learning models and NNPs in general.

Methods

Integration scheme

In this work, we use two neural network potentials of differing complexity to implement a MTS integration scheme. In this scheme, the dynamics of a cheaper NNP is integrated with a small time step (~ 1 fs) and is periodically corrected (every 2 to 6 steps depending on the system) by the force difference between the small NNP and a larger reference model, here the FeNNix-Bio1(M) model.¹⁹ This enables to recover the dynamics of the larger NNP without evaluating its forces at every time step, thus improving the computational efficiency. In particular, we employ the BAOAB-RESPA integration scheme²⁴ outlined in Algorithm 1, that we implemented in the FeNNol library. For simulations in Tinker-HP, we use the

implementation described in²⁴ and the Deep-HP interface²⁶ for calling models.

Algorithm 1 MTS Integration Step with FENNIX Force Splitting

```

1: if first_step then
2:    $F_{\text{small}} \leftarrow \text{FENNIX}_{\text{small}}(x)$ 
3:    $F \leftarrow \text{FENNIX}_{\text{large}}(x)$ 
4: end if
5:  $v \leftarrow v + \frac{\Delta t}{2m} \cdot (F - F_{\text{small}})$ 
6: for  $i = 1$  to  $n_{\text{slow}}$  do
7:    $v \leftarrow v + \frac{\Delta t}{2m \cdot n_{\text{slow}}} \cdot F_{\text{small}}$ 
8:    $x \leftarrow x + \frac{\Delta t}{2 \cdot n_{\text{slow}}} \cdot v$ 
9:    $v \leftarrow \text{thermo}(v, \frac{\Delta t}{n_{\text{slow}}})$  ▷ Apply thermostat
10:   $x \leftarrow x + \frac{\Delta t}{2 \cdot n_{\text{slow}}} \cdot v$ 
11:   $F_{\text{small}} \leftarrow \text{FENNIX}_{\text{small}}(x)$ 
12:   $v \leftarrow v + \frac{\Delta t}{2m \cdot n_{\text{slow}}} \cdot F_{\text{small}}$ 
13: end for
14:  $F \leftarrow \text{FENNIX}_{\text{large}}(x)$ 
15:  $v \leftarrow v + \frac{\Delta t}{2m} \cdot (F - F_{\text{small}})$ 

```

In Algorithm 1, x denotes the system’s coordinates, v its velocities, Δt the outer time step, m the mass and n_{slow} the number of inner steps with time step $\Delta t/n_{\text{slow}}$. $\text{FENNIX}_{\text{large}}(x)$ denotes the reference FeNNix-Bio1(M) machine-learned force field evaluated at configuration x and $\text{FENNIX}_{\text{small}}(x)$ denotes the cheaper model. We describe the neural networks architectures and the distillation strategies employed to train the $\text{FENNIX}_{\text{small}}$ model in the next sections.

Neural Network Architectures

The reference model that we intend to accelerate corresponds to the FeNNix-Bio1(M) model, trained on a broad and diverse dataset. This model is based on a range-separated equivariant transformer architecture where close-range and long-range interactions are described with different spatial resolutions and dedicated attention heads. Its receptive field is 11 Å in total,

via two message-passing interactions. Details about the full architecture are provided in ref.¹⁹ The second, lighter-weight, model that is used in inner steps of the RESPA scheme uses the same base architecture but with reduced capacity and removes the long-range attention heads in order to enable faster inference and lower computational cost. Its receptive field is only 3.5 Å (one message-passing interaction), making it much more short-sighted and allowing it to focus mostly on fast-varying "bonded" forces. The model hyperparameters that we used in the following numerical experiments are provided in Supporting Information.

Training procedures

We derive the FENNIX_{small} model from the reference one via a knowledge distillation procedure^{29,30} where the distilled model is trained on data labeled with the FeNNix-Bio1(M) model instead of DFT. This ensures that the forces used in the inner loop of the RESPA scheme are as close to the reference ones as possible, minimizing the correction necessary to recover the correct dynamics and thus the frequency of its application. In practice, the small model comes in two flavors, either i) as an on-the-fly system-specific model or ii) as a generic model. We briefly describe here these two distillation strategies. Specific details about the training parameters can be found in Supporting Information.

System-specific model For each system, a reference dataset is generated by running a short MD simulation (less than a nanosecond) using the reference model. For proteins and, more generally, for large systems, a fragmentation strategy similar to the one proposed in ref.³¹ was employed to reduce the computational burden while retaining local structural information. We then evaluate the energies and forces of the collected frames with the reference model. The on-the-fly system-specific model is then trained on this dataset, resulting in a model about 10 times faster than FeNNix-Bio1(M) with our current setup.

Generic model In addition to system-specific distilled models, we also propose a generic fast model trained on a chemically diverse dataset, enabling broader applicability and faster

deployment in new systems. To construct this transferable potential, we generate a training set by evaluating FeNNix-Bio1(M) on a subset of conformations from the SPICE2 dataset,^{32,33} which contains a wide variety of small organic molecules and biologically-relevant complexes. The generic model is trained on the obtained dataset, resulting in a transferable model that captures general chemical patterns and can be reused across systems. This generic model can be used directly in the inner loop of our MTS scheme, or serve as an initialization point for further fine-tuning on a target system. This offers a compromise between generality and accuracy, especially when system-specific data is limited or a rapid deployment is desired.

Numerical experiments

The results obtained with the MTS scheme for each of the following experiments are compared to a single time step (STS) integrator using the FeNNix-Bio1(M) force field with a time step of 1 fs. The STS scheme employs a BAOAB Langevin integrator.^{34,35}

Bulk Water

First, to investigate the robustness of our models and integrator, we performed a series of stability tests on a small water box containing 648 atoms. Simulations were carried out using the system-specific model and the generic model, with external time steps ranging from 2 fs to 9 fs. For each configuration, we monitored dynamical and thermodynamical observables, including diffusion coefficients, kinetic and potential energies, and temperature. Diffusion coefficients were computed using Tinker³⁶ with the Einstein formula. The stability of the trajectory was evaluated over the full course of the 2 ns simulation, with qualitative indicators reported in table 1. Additional tests were performed with hydrogen mass repartitioning (HMR), enabling larger time steps.

At short external time step (2 fs), both specific and generic model produced stable tra-

Table 1: Stability tests performed on a water box of 648 atoms using both the system-specific and generic models at various integration time steps, with and without hydrogen mass repartitioning (HMR). Diffusion coefficients (in 10^{-5} cm²/s) and average temperatures (K) are reported with associated standard deviations. Values are averaged over 2 ns trajectories. Instabilities prevented completion of simulations beyond 3 fs without HMR and beyond 7 fs with HMR.

	Diffusion		Temperature	
	System	Generic	System	Generic
STS		2.2		300.1±9.6
2 fs	2.2	2.1	300.5±9.6	300.2±9.6
3 fs	2.3	2.6	315.2±10.6	333.3±12.2
4 fs HMR	2.2	2.4	300.8±9.5	303.4±9.9
5 fs HMR	2.3	2.5	302.7±9.8	304.1±10.2
6 fs HMR	2.5	2.0	304.5±9.7	305.9±9.9
7 fs HMR	NaN	3.3	NaN	327.5±11.1

jectories with diffusion coefficients and temperatures close to the reference STS values. At 3 fs, simulations remained stable, though the generic and system-specific model displayed a marked increase in both diffusion coefficient and temperature, suggesting the onset of integration artifacts.

The introduction of HMR enables stable simulations up to 6 fs, with dynamical and thermodynamical properties remaining within reasonable agreement between STS and MTS integrator for both models. However, at 7 fs and beyond, instabilities systematically occurred, reflected by divergent values in Table 1 or nonphysical increase in diffusion and temperature. These results highlight that HMR provides a substantial extension of the accessible time step, effectively doubling the stability range compared to standard masses. Nevertheless, care must be taken to avoid excessive increases as instabilities rapidly emerge beyond 6 fs. In practice, time steps of 2 fs to 3 fs without HMR, and up to 5-6 fs with HMR, appear to offer the most reliable compromise between computational efficiency, stability, and physical accuracy.

It is well documented that limits in the larger time step usable in the context of MTS schemes in molecular dynamics are related to the coupling of this largest time step with the highest-frequency vibrational modes involved in the system: the so-called resonance

effects.^{37–44} A simple diagnostic can be made to assess these aspects by considering the velocity autocorrelation spectra in this setup. Figure 1 illustrates this in the context of bulk water where we see the artifacts produced by the periodic MTS force correction (annotated in the inset of Figure 1) progressively coupling with the overtone of the O-H stretching mode (around 7500 cm^{-1} or 4000 cm^{-1} with HMR) as the outer time step increases. This diagnostic confirms the limits of the outer time step to 5 fs with hydrogen mass repartitioning and 2-3 fs without.

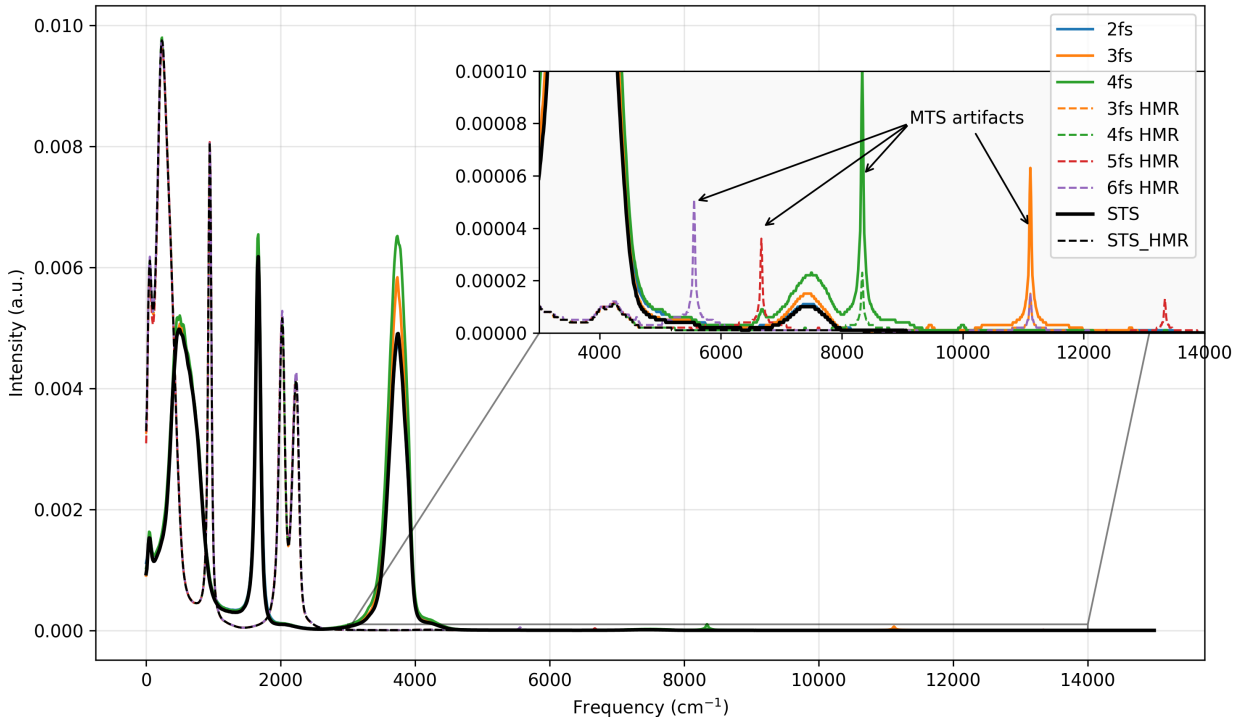


Figure 1: Average velocity autocorrelation spectra of hydrogen atoms for bulk water. The reference single time step (STS) simulation are shown in black. Multi time step (MTS) simulations are shown for different integration time steps (2 fs, 3 fs, 4 fs, 5 fs, and 6 fs), with corresponding heavy-mass repartitioning (HMR) variants represented by dashed lines of the same color. Insets zoom in high frequency regions containing MTS integration artifacts.

We further assess the robustness of our approach by computing the radial distribution function of bulk water. As shown in Figure 2, the MTS simulations (with both generic and system-specific models) with an outer time step of 5 fs and HMR correctly reproduce the STS results within statistical uncertainties. Overall, with this setup, we obtain a speedup of

around 4 compared to STS with 1 fs time step for bulk water simulations.

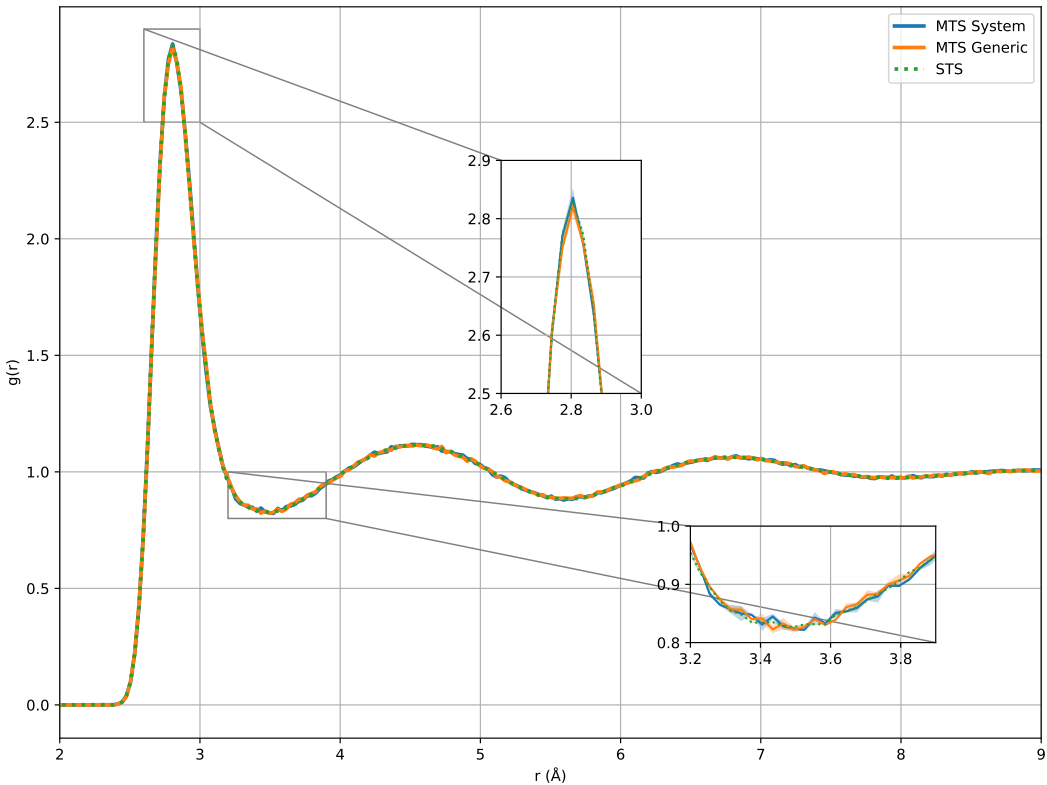


Figure 2: Radial distribution function, $g(r)$, as a function of the distance (r) in Å. The solid blue curve corresponds to the MTS simulation with the on-the-fly system-specific model and the orange one to MTS with the small generic model. Both MTS simulations used an inner time step of 1 fs and an outer time step of 5 fs. The dotted green curve corresponds to the reference STS simulation.

Solvated Molecules

To further assess the accuracy of the proposed MTS scheme, we turn to small solvated molecules. We observe stability limits similar to those for bulk water for the five molecules that we tested: ethanol, benzene, trimethylamine, diethylsulfide, and acetic acid. We then evaluated the hydration free energies (HFEs) of these (as well as water). Calculations were performed leveraging the alchemical Lambda-ABF⁴⁵ method, employing both system-specific models trained on-the-fly and a generic small foundation model. All simulations were carried out using the same MTS integration scheme described above, with an inner time step of 1 fs

and an outer time step of 3 fs.

The predicted HFEs were compared to the STS reference values, as shown in Figure 3. The system-specific model achieved a mean absolute error (MAE) of 0.152 kcal/mol, a root-mean-square error (RMSE) of 0.206 kcal/mol, and a coefficient of determination (R^2) of 0.991. The generic foundation model also showed good performance, with an MAE of 0.222 kcal/mol, an RMSE of 0.268 kcal/mol, and R^2 of 0.984.

These results demonstrate that the MTS scheme preserves high accuracy in free energy calculations while benefiting from a significant reduction in computational cost. They also show that both system-specific and generic models are capable of closely reproducing STS-level results.

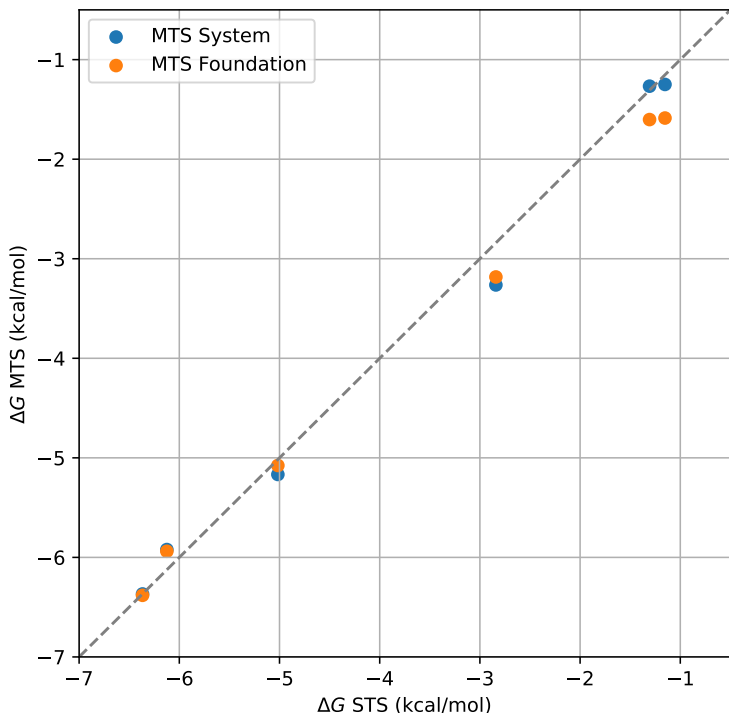


Figure 3: Hydration free energy of small molecules (water, ethanol, benzene, trimethylamine, diethylsulfide and acetic acid) using MTS with system-specific model, blue points, and with small foundation model, orange points, compared to the STS reference method. MAE is 0.152 kcal/mol and 0.222 kcal/mol, RMSE is 0.206 kcal/mol and 0.268 kcal/mol, R^2 is 0.991 and 0.984 for respectively the system-specific model and the small foundation model.

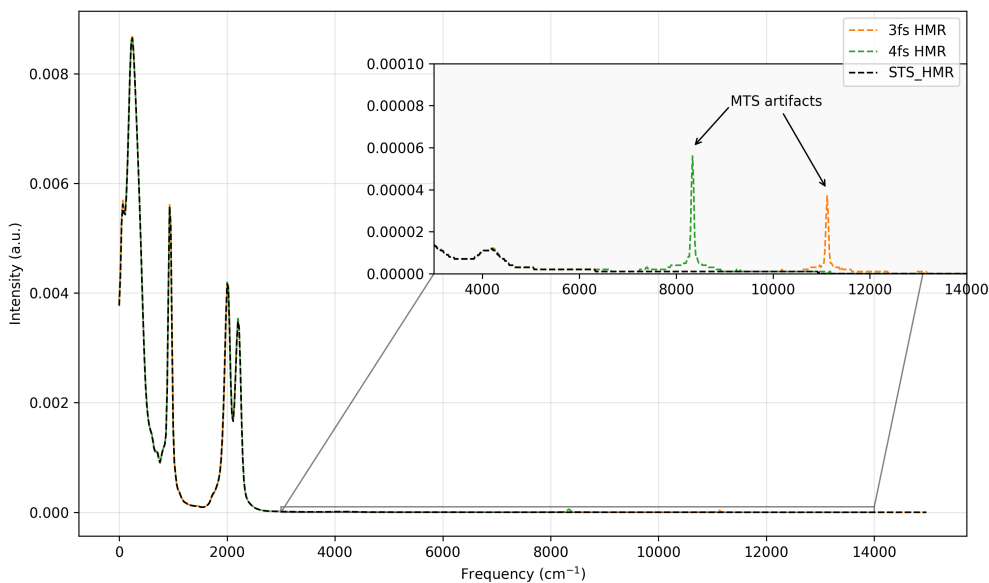
Protein-ligand complexes

To validate our scheme on a biologically relevant system, we performed a 20 ns NVT molecular dynamics simulation of the lysozyme–phenol complex (PDB ID: 4I7L) in explicit water. We first resorted to a setup of 4 fs outer time step and HMR which is stable for bulk water, but this led to instabilities after 2 ns of simulation. Figure 4a shows the velocity autocorrelation spectra computed over a short simulation with both STS and MTS with HMR enabled. The close similarity of the obtained spectra indicates that the instabilities are not due to the resonance phenomena described above.

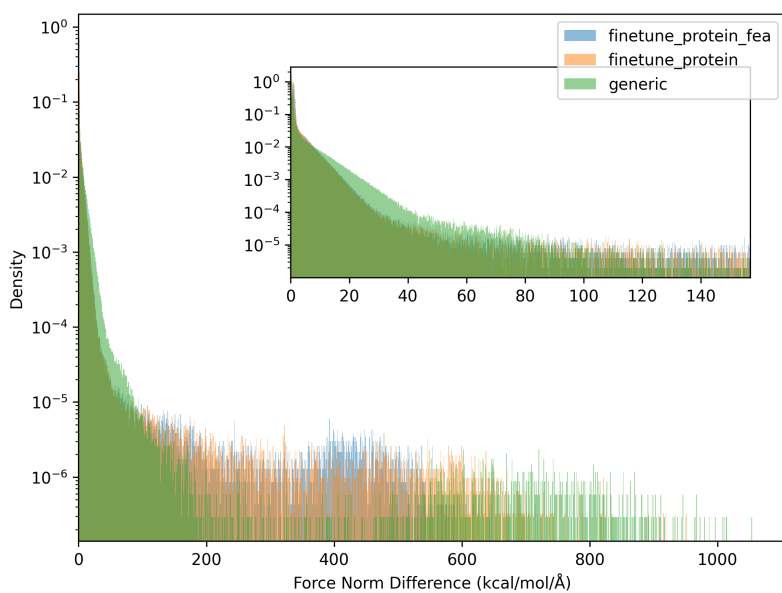
In practice, this source of instability lies in the presence of "holes" in the potential energy surface of the small model, yielding large differences between its forces and the target ones. This is illustrated in Figure 4b showing the distribution of the norm of the difference of forces between FeNNix-Bio1(M) and the distilled model (either finetuned on system-specific fragments or the generic one) along an STS trajectory of the protein-ligand system. We observe a dense distribution of values close to 0 kcal/mol/Å and a long tailed distribution starting from 150 kcal/mol/Å. The latter is associated to large nonphysical force discrepancies yielding the infrequent instabilities that we observe in the MTS simulation.

We attempted to mitigate this issue by clipping the force difference to exclude unrealistic values while preserving the meaningful ones (in practice, we used a threshold of 150 kcal/mol/Å on force components). While improving the stability, this setup still leads to the rare occurrence of crashes due to large differences when the time step is equal to or larger than 4 fs. We expect that an active learning loop where the "holes" are first identified and then included in a fine-tuning stage will systematically improve the stability of our MTS scheme with larger time steps; this will be the focus of a future work.

Using an inner time step of 1.5 fs and an outer time step of 3 fs with HMR, stable simulations over 20 ns were obtained while preserving the protein’s structure and the ligand’s binding mode as shown in Figure 5. This setup provides a speedup of 2.3 with respect to the STS simulation with 1 fs time step, strongly accelerating production simulations with



(a) velocity autocorrelation spectrum



(b) Distribution of the force difference

Figure 4: a) Average velocity autocorrelation spectra of hydrogen atoms for the phenol-lysozyme complex with HMR, comparing STS with MTS 3 fs and 4 fs. Insets zoom in high frequency regions containing MTS integration artifacts. b) Distribution (in log-scale) of the norm of the force differences for the generic model, the fine-tuned model trained on forces, energies, and atomic energies, and the fine-tuned model trained on forces and energy, with respect to the FENNIX-Bio1(M) reference model. The distributions are estimated over the first 500 frames of a phenol-lysozyme in water simulation.

biological systems.

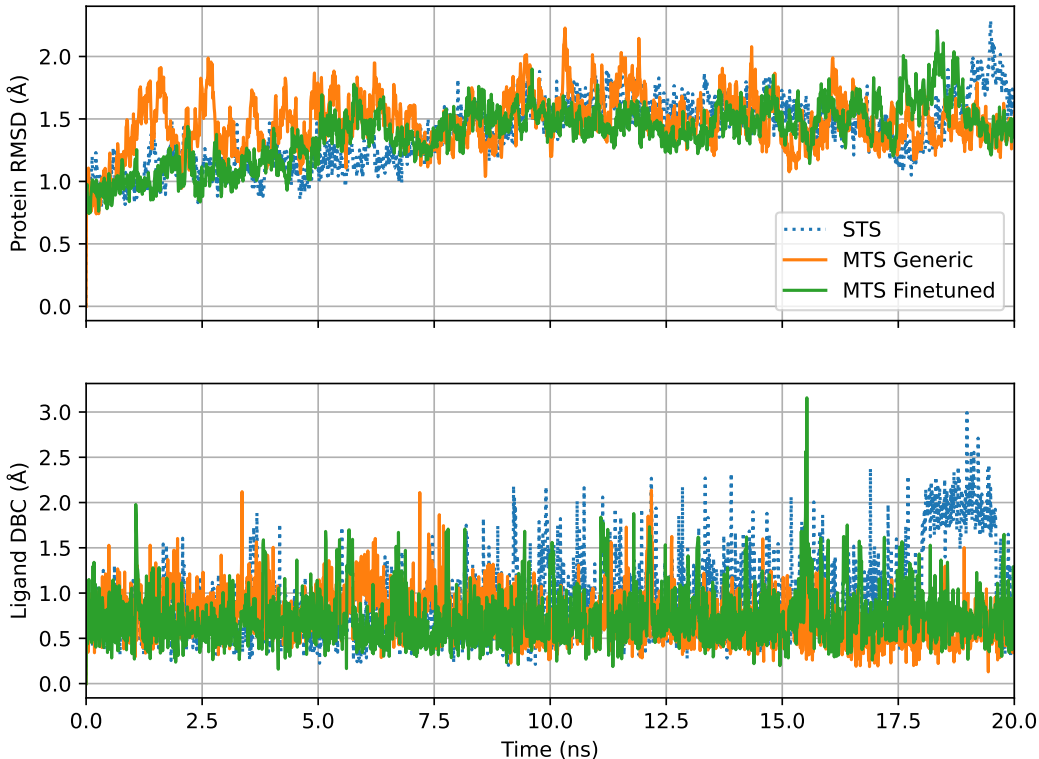


Figure 5: Time evolution of the protein backbone RMSD and the ligand’s Distance to Bound Configuration (DBC)⁴⁶ during a 20 ns simulation of the lysozyme–phenol complex in water. Results obtained with the implemented MTS integrator (solid lines) are compared to those from a reference STS simulation (dotted lines). MTS simulations use either the generic or finetuned models combined with the FeNNix-Bio1(M) potential with an internal time step of 1.5 fs and an external time step of 3 fs with HMR.

Conclusion

We have introduced a practical and efficient Multiple Time Step (MTS) scheme tailored to machine-learned force fields, enabling significant acceleration of molecular dynamics simulations without compromising accuracy for both static and dynamical properties. Our approach, based on a RESPA-like scheme, couples a fast, distilled neural network model with the accurate FeNNix-Bio1(M) reference potential. We demonstrated two complementary distillation strategies: (i) on-the-fly system-specific model distillation, and (ii) the use

of a lightweight transferable model for broader applicability.

We achieve substantial speedups – up to 4 in mostly homogeneous systems (bulk water and solvated small molecules) and 2.3 in large protein-ligand complexes – while preserving key physical observables such as radial distribution functions, hydration free energies, diffusion coefficients, and protein-ligand structural properties. Note that this is a first estimation of the computational gains as the code has yet to be optimized further to handle the dual-level approach more efficiently. All in all, our approach allows to reach nearly 6 ns of simulation per day on a single A100 GPU for a realistic protein-ligand complex while preserving the *ab initio*-like accuracy of the FeNNix-Bio1(M) model. In combination with well-established accelerated sampling schemes,^{47–49} this enables truly large-scale simulations with foundation neural neural network potentials.

Future work will focus on expanding the applicability of this approach through two main avenues. First, randomized time stepping could be explored to further increase the effective time step, while allowing for controlled velocity rescaling as proposed in stochastic RESPA variants, i.e. JUMP integrators.⁴⁴ Second, system-specific models can be fine-tuned more efficiently using fragment-based active-learning strategies to progressively fill-out "holes" in the small model's potential energy surface, potentially improving stability with even larger time steps for more complex chemical systems.

Acknowledgments

This work has received funding from the European Research Council (ERC) under the European Union's Horizon 2020 research and innovation program (grant agreement No 810367), project EMC2 (JPP). Computations have been performed at IDRIS (Jean Zay) on GENCI Grants: no A0150712052 (J.-P. P.).

References

- (1) Behler, J.; Parrinello, M. Generalized neural-network representation of high-dimensional potential-energy surfaces. *Physical Review Letters* **2007**, *98*, 146401.
- (2) Bartók, A. P.; Payne, M. C.; Kondor, R.; Csányi, G. Gaussian approximation potentials: The accuracy of quantum mechanics, without the electrons. *Physical Review Letters* **2010**, *104*, 136403.
- (3) Chmiela, S.; Sauceda, H. E.; Müller, K.-R.; Tkatchenko, A. Towards exact molecular dynamics simulations with machine-learned force fields. *Nature Communications* **2018**, *9*, 1–10.
- (4) Shakouri, K.; Behler, J.; Meyer, J.; Kroes, G.-J. Accurate neural network description of surface phonons in reactive gas–surface dynamics: N₂+ Ru (0001). *The journal of physical chemistry letters* **2017**, *8*, 2131–2136.
- (5) Smith, J. S.; Isayev, O.; Roitberg, A. E. ANI-1: an extensible neural network potential with DFT accuracy at force field computational cost. *Chemical Science* **2017**, *8*, 3192–3203.
- (6) Schütt, K.; Kindermans, P.-J.; Sauceda Felix, H. E.; Chmiela, S.; Tkatchenko, A.; Müller, K.-R. Schnet: A continuous-filter convolutional neural network for modeling quantum interactions. *Advances in neural information processing systems* **2017**, *30*.
- (7) Unke, O. T.; Chmiela, S.; Gastegger, M.; Schütt, K. T.; Sauceda, H. E.; Müller, K.-R. SpookyNet: Learning force fields with electronic degrees of freedom and nonlocal effects. *Nature Communications* **2021**, *12*, 1–14.
- (8) Gasteiger, J.; Becker, F.; Günnemann, S. Gemnet: Universal directional graph neural networks for molecules. *Advances in Neural Information Processing Systems* **2021**, *34*, 6790–6802.

- (9) Musaelian, A.; Batzner, S.; Johansson, A.; Sun, L.; Owen, C. J.; Kornbluth, M.; Kozinsky, B. Learning local equivariant representations for large-scale atomistic dynamics. *Nature Communications* **2023**, *14*, 579.
- (10) Grisafi, A.; Ceriotti, M. Incorporating long-range physics in atomic-scale machine learning. *The Journal of Chemical Physics* **2019**, *151*, 204105.
- (11) Devereux, C.; Smith, J. S.; Huddleston, K. K.; Barros, K.; Zubatyuk, R.; Isayev, O.; Roitberg, A. E. Extending the Applicability of the ANI Deep Learning Molecular Potential to Sulfur and Halogens. *Journal of Chemical Theory and Computation* **2020**, *16*, 4192–4202.
- (12) Zubatyuk, R.; Smith, J. S.; Leszczynski, J.; Isayev, O. Accurate and transferable multitask prediction of chemical properties with an atoms-in-molecules neural network. *Science Advances* **2019**, *5*, eaav6490.
- (13) Grisafi, A.; Nigam, J.; Ceriotti, M. Multi-scale approach for the prediction of atomic scale properties. *Chemical Science* **2021**, *12*, 2078–2090.
- (14) Kabylda, A.; Frank, J. T.; Suárez-Dou, S.; Khabibrakhmanov, A.; Medrano Sandonas, L.; Unke, O. T.; Chmiela, S.; Müller, K.-R.; Tkatchenko, A. Molecular Simulations with a Pretrained Neural Network and Universal Pairwise Force Fields. *Journal of the American Chemical Society* **2025**, *147*, 33723–33734, DOI: 10.1021/jacs.5c09558, PMID: 40886167.
- (15) Unke, O. T.; Stöhr, M.; Ganscha, S.; Untertiner, T.; Maennel, H.; Kashubin, S.; Ahlin, D.; Gastegger, M.; Sandonas, L. M.; Berryman, J. T.; Tkatchenko, A.; Müller, K.-R. Biomolecular dynamics with machine-learned quantum-mechanical force fields trained on diverse chemical fragments. *Science Advances* **2024**, *10*, eadn4397, DOI: 10.1126/sciadv.adn4397.

- (16) Batatia, I.; Kovacs, D. P.; Simm, G.; Ortner, C.; Csányi, G. MACE: Higher order equivariant message passing neural networks for fast and accurate force fields. *Advances in Neural Information Processing Systems* **2022**, *35*, 11423–11436.
- (17) Kovács, D. P.; Moore, J. H.; Browning, N. J.; Batatia, I.; Horton, J. T.; Pu, Y.; Kapil, V.; Witt, W. C.; Magdău, I.-B.; Cole, D. J.; Csányi, G. MACE-OFF: Short-Range Transferable Machine Learning Force Fields for Organic Molecules. *Journal of the American Chemical Society* **2025**, *147*, 17598–17611, DOI: 10.1021/jacs.4c07099, PMID: 40387214.
- (18) Plé, T.; Lagardère, L.; Piquemal, J.-P. Force-field-enhanced neural network interactions: from local equivariant embedding to atom-in-molecule properties and long-range effects. *Chemical Science* **2023**, *14*, 12554–12569, DOI: 10.1039/D3SC02581K.
- (19) Plé, T.; Adjoua, O.; Benali, A.; Posenitskiy, E.; Villot, C.; Lagardère, L.; Piquemal, J.-P. A Foundation Model for Accurate Atomistic Simulations in Drug Design. *ChemRxiv* **2025**, DOI: 10.26434/chemrxiv-2025-f1hgn-v3.
- (20) Benali, A. et al. Pushing the Accuracy Limit of Foundation Neural Network Models with Quantum Monte Carlo Forces and Path Integrals. *preprint arXiv:2504.07948* **2025**,
- (21) MacKerell, A. D. Chapter 7 Empirical Force Fields for Proteins: Current Status and Future Directions. 2005; <https://www.sciencedirect.com/science/article/pii/S1574140005010078>.
- (22) Tuckerman, M.; Berne, B. J.; Martyna, G. J. Reversible multiple time scale molecular dynamics. *The Journal of Chemical Physics* **1992**, *97*, 1990–2001, DOI: 10.1063/1.463137.
- (23) Zhou, R.; Harder, E.; Xu, H.; Berne, B. Efficient multiple time step method for use with Ewald and particle mesh Ewald for large biomolecular systems. *The Journal of chemical physics* **2001**, *115*, 2348–2358.

- (24) Lagardère, L.; Aviat, F.; Piquemal, J.-P. Pushing the limits of multiple-time-step strategies for polarizable point dipole molecular dynamics. *The journal of Physical Chemistry Letters* **2019**, *10*, 2593–2599.
- (25) Plé, T.; Adjoua, O.; Lagardère, L.; Piquemal, J.-P. FeNNol: An efficient and flexible library for building force-field-enhanced neural network potentials. *The Journal of Chemical Physics* **2024**, *161*, 042502, DOI: 10.1063/5.0217688.
- (26) Jaffrelot Inizan, T.; Plé, T.; Adjoua, O.; Ren, P.; Gokcan, H.; Isayev, O.; Lagardère, L.; Piquemal, J.-P. Scalable hybrid deep neural networks/polarizable potentials biomolecular simulations including long-range effects. *Chemical Science* **2023**, *14*, 5438–5452, DOI: 10.1039/D2SC04815A.
- (27) Lagardère, L.; Jolly, L.-H.; Lipparini, F.; Aviat, F.; Stamm, B.; Jing, Z. F.; Harger, M.; Torabifard, H.; Cisneros, G. A.; Schnieders, M. J.; Gresh, N.; Maday, Y.; Ren, P. Y.; Ponder, J. W.; Piquemal, J.-P. Tinker-HP: a massively parallel molecular dynamics package for multiscale simulations of large complex systems with advanced point dipole polarizable force fields. *Chemical Science* **2018**, *9*, 956–972, DOI: 10.1039/C7SC04531J.
- (28) Adjoua, O.; Lagardère, L.; Jolly, L.-H.; Durocher, A.; Very, T.; Dupays, I.; Wang, Z.; Jaffrelot Inizan, T.; Célerse, F.; Ren, P.; Ponder, J. W.; Piquemal, J.-P. Tinker-hp: Accelerating molecular dynamics simulations of large complex systems with advanced point dipole polarizable force fields using gpus and multi-gpu systems. *Journal of Chemical Theory and Computation* **2021**, *17*, 2034–2053.
- (29) Hinton, G.; Vinyals, O.; Dean, J. Distilling the knowledge in a neural network. *arXiv preprint arXiv:1503.02531* **2015**,
- (30) Gou, J.; Yu, B.; Maybank, S. J.; Tao, D. Knowledge distillation: A survey. *International journal of computer vision* **2021**, *129*, 1789–1819.

- (31) Unke, O. T.; Stöhr, M.; Ganscha, S.; Untertiner, T.; Maennel, H.; Kashubin, S.; Ahlin, D.; Gastegger, M.; Sandonas, L. M.; Berryman, J. T.; Tkatchenko, A.; Müller, K.-R. Biomolecular dynamics with machine-learned quantum-mechanical force fields trained on diverse chemical fragments. *Science Advances* **2024**, *10*, eadn4397, DOI: 10.1126/sciadv.adn4397.
- (32) Eastman, P.; Behara, P. K.; Dotson, D. L.; Galvelis, R.; Herr, J. E.; Horton, J. T.; Mao, Y.; Chodera, J. D.; Pritchard, B. P.; Wang, Y.; others SPICE, A Dataset of Drug-like Molecules and Peptides for Training Machine Learning Potentials. *Scientific Data* **2023**, *10*, 11.
- (33) Eastman, P.; Pritchard, B. P.; Chodera, J. D.; Markland, T. E. Nutmeg and SPICE: Models and Data for Biomolecular Machine Learning. *Journal of Chemical Theory and Computation* **2024**, *20*, 8583–8593.
- (34) Leimkuhler, B.; Matthews, C. Rational Construction of Stochastic Numerical Methods for Molecular Sampling. *Applied Mathematics Research eXpress* **2012**, *2013*, 34–56, DOI: 10.1093/amrx/abs010.
- (35) Leimkuhler, B.; Matthews, C. Rational construction of stochastic numerical methods for molecular sampling. *Applied Mathematics Research eXpress* **2013**, *2013*, 34–56.
- (36) Rackers, J. A.; Wang, Z.; Lu, C.; Laury, M. L.; Lagardère, L.; Schnieders, M. J.; Piquemal, J.-P.; Ren, P.; Ponder, J. W. Tinker 8: software tools for molecular design. *Journal of chemical theory and computation* **2018**, *14*, 5273–5289.
- (37) Biesiadecki, J. J.; Skeel, R. D. Dangers of Multiple Time Step Methods. *Journal of Computational Physics* **1993**, *109*, 318 – 328.
- (38) Ma, Q.; Izaguirre, J.; Skeel, R. Verlet-I/R-RESPA/Impulse is Limited by Nonlinear Instabilities. *SIAM Journal on Scientific Computing* **2003**, *24*, 1951–1973, DOI: 10.1137/S1064827501399833.

- (39) Morrone, J. A.; Markland, T. E.; Ceriotti, M.; Berne, B. J. Efficient multiple time scale molecular dynamics: Using colored noise thermostats to stabilize resonances. *The Journal of Chemical Physics* **2011**, *134*, 014103, DOI: 10.1063/1.3518369.
- (40) Leimkuhler, B.; Margul, D. T.; Tuckerman, M. E. Stochastic, resonance-free multiple time-step algorithm for molecular dynamics with very large time steps. *Molecular Physics* **2013**, *111*, 3579–3594.
- (41) Margul, D. T.; Tuckerman, M. E. A Stochastic, Resonance-Free Multiple Time-Step Algorithm for Polarizable Models That Permits Very Large Time Steps. *Journal of Chemical Theory and Computation* **2016**, *12*, 2170–2180, DOI: 10.1021/acs.jctc.6b00188.
- (42) Albaugh, A.; Tuckerman, M. E.; Head-Gordon, T. Combining Iteration-Free Polarization with Large Time Step Stochastic-Isokinetic Integration. *Journal of Chemical Theory and Computation* **2019**, *15*, 2195–2205, DOI: 10.1021/acs.jctc.9b00072.
- (43) Gouraud, N.; Bris, P. L.; Majka, A.; Monmarché, P. HMC and Underdamped Langevin United in the Unadjusted Convex Smooth Case. *SIAM/ASA Journal on Uncertainty Quantification* **2025**, *13*, 278–303, DOI: 10.1137/23M1608963.
- (44) Gouraud, N.; Lagardère, L.; Adjoua, O.; Plé, T.; Monmarché, P.; Piquemal, J.-P. Velocity Jumps for Molecular Dynamics. *Journal of Chemical Theory and Computation* **2025**, *21*, 2854–2866, DOI: 10.1021/acs.jctc.5c00023.
- (45) Lagardère, L.; Maurin, L.; Adjoua, O.; El Hage, K.; Monmarché, P.; Piquemal, J.-P.; Hénin, J. Lambda-ABF: Simplified, Portable, Accurate, and Cost-Effective Alchemical Free-Energy Computation. *Journal of Chemical Theory and Computation* **2024**, *20*, 4481–4498.
- (46) Salari, R.; Joseph, T.; Lohia, R.; Hénin, J.; Brannigan, G. A streamlined, general approach for computing ligand binding free energies and its application to GPCR-bound cholesterol. *Journal of chemical theory and computation* **2018**, *14*, 6560–6573.

- (47) Célerse, F.; Inizan, T. J.; Lagardère, L.; Adjoua, O.; Monmarché, P.; Miao, Y.; Derat, E.; Piquemal, J.-P. An Efficient Gaussian-Accelerated Molecular Dynamics (GaMD) Multilevel Enhanced Sampling Strategy: Application to Polarizable Force Fields Simulations of Large Biological Systems. *Journal of Chemical Theory and Computation* **2022**, *18*, 968–977, DOI: 10.1021/acs.jctc.1c01024.
- (48) Jaffrelot Inizan, T.; Célerse, F.; Adjoua, O.; El Ahdab, D.; Jolly, L.-H.; Liu, C.; Ren, P.; Montes, M.; Lagarde, N.; Lagardère, L.; Monmarché, P.; Piquemal, J.-P. High-resolution mining of the SARS-CoV-2 main protease conformational space: supercomputer-driven unsupervised adaptive sampling. *Chemical Science* **2021**, *12*, 4889–4907.
- (49) Ansari, N.; Jing, Z. F.; Gagelin, A.; Hédin, F.; Aviat, F.; Hénin, J.; Piquemal, J.-P.; Lagardère, L. Lambda-ABF-OPES: Faster Convergence with High Accuracy in Alchemical Free Energy Calculations. *The Journal of Physical Chemistry Letters* **2025**, *16*, 4626–4634, DOI: 10.1021/acs.jpcllett.5c00683, PMID: 40312308.